proposed[12] for the β-avoparcin-Ac_2-Lys-D-Ala-D-Ala complex and a more recent report[13] on the structure of the ristocetin-tripeptide complex in aqueous solution in which the lysine side chain is over the D ring of the antibiotic.

From a quantitative analysis of our NOE data, it was concluded that no one structure could fit all of the NMR data. By including an additional pseudobond term in the force field used to model the complex, we were able to produce a structure which agreed with the observed proton-proton distances included as constraints. Relaxing the pseudobond constraint, however, produced a structure with several distances not in accord with observations. Through the use of molecular dynamics calculations, additional structures were generated which compared more favorably to the NOE derived distances. By obtaining many proton-proton distances as accurately as possible and employing molecular dynamics calculations, dynamic averaging effects were considered in the interpretation of the measured NMR parameters. These methods allowed us to obtain detailed structural information which may prove to be important in the rational design of pharmaceutical agents. The general methodology described here is currently being refined and applied in structural studies of other physiologically important molecules.[29]

Acknowledgment. The authors thank E. R. P. Zuiderweg for writing the 2D base line correction routine used in the data processing and G. Bolis for modifying the VFF program to include the NOE derived distance constraints.

(29) Fesik, S. W.; Holleman, W. H.; Perun, T. J. *Biochem. Biophys. Res. Commun.* **1985**, *131*, 517.
(30) Tropp, J. *J. Chem. Phys.* **1980**, *72*, 6035.
(31) Bystrov, V. F. In *Progress in NMR Spectroscopy*; Pergamon Press: Great Britain, 1976; Vol. 10, pp 41-81.

Optical Detection of Paramagnetic Resonance by Magnetic Circular Dichroism. Applications to Aqueous Solutions of Metalloproteins

Christopher P. Barrett,[†] Jim Peterson,[†] Colin Greenwood,[‡] and Andrew J. Thomson*[†]

Contribution from the School of Chemical Sciences and School of Biological Sciences, University of East Anglia, Norwich NR4 7TJ, U.K. *Received September 9, 1985*

Abstract: An apparatus has been assembled to enable microwave resonance of a ground electronic state to be detected by measuring the intensity of the magnetic circular dichroism (MCD) spectrum. The sample is mounted in a rectangular *Q*-band cavity resonating in the TE_{102} mode which can be lowered into the center of a split-coil superconducting magnet. The circular dichroism signal is measured with a JASCO-J500D spectropolarimeter, a monochromatic optical beam of differentially circularly polarized light being passed along the magnetic field axis of the solenoid and through the microwave cavity. This apparatus has been used to measure the MCD-detected optical double microwave resonance (ODMR) of frozen aqueous solutions of Cu^{II}(EDTA) and copper(II) azurin, a blue copper protein obtained from *Pseudomonas aeruginosa*. The line shapes of the MCD-ODMR spectrum are the same as in the *Q*-band EPR spectrum only in the case that the optical transition is isotropic, as appears to be the case for Cu^{II}(EDTA). The MCD-ODMR spectrum of azurin has been measured at four optical wavelengths, 460, 640, 750, and 1000 nm, corresponding to the positions of the major features in the MCD spectrum. These bands arise from charge-transfer transitions from cysteine and histidine ligand-to-copper(II) $d_{x^2-y^2}$ orbitals. The MCD-ODMR detects only the *z* component of the ground-state *g* tensor. A simple computer simulation shows that this implies that the MCD transitions at these wavelengths arise from *x,y*-polarized bands. The shapes of the MCD-ODMR lines hence provide a method of determining the polarizations of optical transitions relative to one another and to the ground-state *g*-tensor axes of a paramagnetic species in frozen solutions. The MCD spectrum can be partially quenched by application of microwave power when the microwave photon energy is equal to the ground-state Zeeman energy. In this way it is possible to deconvolute the MCD spectrum of a chromophore even though several different species are present with overlapping optical spectra. This appears to be the first application of the technique of MCD-ODMR to frozen aqueous solutions and to the study of metalloproteins. The technique promises to yield much useful information about the electronic and molecular structure of transition-metal ions in proteins.

Low-temperature magnetic circular dichroism (MCD) spectroscopy is now well established as a useful optical probe of the ground-state magnetic properties of metal centers in metalloproteins.[1-3] Using suitable mixtures of glassing agents, aqueous solutions of protein can be cooled to liquid helium temperatures, yielding samples of sufficiently good optical quality to enable reliable MCD spectra to be measured. Paramagnetic metal centers give temperature- and magnetic field-dependent MCD signals in the region of their optical absorption bands. The temperature dependence is a consequence of the Boltzmann population distribution among the Zeeman-split sublevels which results in the differential absorption of left-minus-right circularly polarized light.[4] A plot of the intensity of the MCD signal at a fixed wavelength against B/T, where B is the magnetic field and T the absolute temperature, constitutes a magnetization curve. Analysis of the form of the curve in favorable cases enables the ground-state *g* values and spin S to be determined.[1] An optical probe of

[†] School of Chemical Sciences.
[‡] School of Biological Sciences.

(1) Thomson, A. J.; Johnson, M. K. *Biochem. J.* **1980**, *191*, 411.
(2) For a recent review of results on metalloproteins, excluding heme, see: (a) Johnson, M. K.; Robinson, A. E.; Thomson, A. J. In *Iron Sulfur Proteins*; Spiro, T. G., *Ed.*; Wiley: New York 1982; Vol. 4, Chapter 10. (b) Dooley, D. M.; Dawson, J. H. *Coord. Chem. Rev.* **1984**, *60*, 1.
(3) For examples of applications to heme-containing systems, see: (a) Walsh, T. A.; Johnson, M. K.; Greenwood, C.; Barber, D.; Springall, J. P. *Biochem. J.* **1979**, *177*, 29. (b) Thomson, A. J.; Johnson, M. K., Greenwood, C.; Gooding, P. E. *Biochem. J.* **1981**, *193*, 687. (c) Brittain, T.; Greenwood, C.; Springall, J. P.; Thomson, A. J. *Biochim. Biophys. Acta* **1982**, *703*, 117. (d) Thomson, A. J.; Eglinton, D. G.; Hill, B. C.; Greenwood, C. *Biochem. J.* **1982**, *207*, 167.
(4) Stephens, P. J. *Adv. Chem. Phys.* **1976**, *35*, 197.

0002-7863/86/1508-3170$01.50/0

paramagnetism has proved to be especially valuable for the study of complex metalloproteins that contain more than one metal center or for proteins containing an EPR silent paramagnet. Determination of the MCD magnetization curves at different wavelengths enables each band in the optical spectrum to be assigned to a given signal in the electron paramagnetic resonance (EPR) spectrum. Conversely use of the ground-state g values as determined from EPR measurements allows the form of the MCD magnetization curve to be predicted and hence bands in the optical spectrum to be assigned to given centers. For example, the optical transitions of the copper ion which is EPR detectable in resting, oxidized state of cytochrome *c* oxidase, have been deconvoluted from the low-temperature MCD spectrum of the enzyme even though they are overlaid by those arising from the heme centers.[5] One of the limitations, however, arises in the case of paramagnetic centers with anisotropic ground-state g tensors. The analysis of MCD magnetization curves relies upon the fitting of multiparameter expressions, and g-factor anisotropy increases the number of parameters. Thus, it is rarely possible to determine g-factor anisotropies from an analysis of MCD magnetization curves. In addition the technique is relatively crude as a method of determining ground-state g values, and it is not really possible to distinguish between paramagnets of closely similar g values with the same discriminating power as magnetic resonance can provide.

These disadvantages can be overcome and the technique extended in a number of important ways by using the MCD signal to detect microwave resonance in the ground state. This experiment is a form of optically detected magnetic resonance (ODMR).[6] Although ODMR spectroscopy has found increasing application to problems of biological interest, it has been almost exclusively concerned with the properties of the excited triplet states of organic molecules. There have been only a few reports of the use of magnetic circular dichroism to detect microwave resonance signals, and they all involve applications to the study of transition-metal ions doped into ionic crystals or of color centers in crystal lattices and, more recently, of defect sites in semiconductors. The MCD bands associated with the F^+ color center in SrO were used to detect the paramagnetic resonance and hence to distinguish the optical bands of this center from those of a Mn^{2+} impurity.[7] The MCD signals of the $^6S \rightarrow {}^4T_2$ transition of Mn^{2+} doped into a single crystal of the spinel $MgO{\cdot}3Al_2O_3$ enabled the paramagnetic resonance of the ground state to be detected at microwave frequencies of 19.1 and 24.1 GHz.[8] Broad paramagnetic resonance signals corresponding to transitions at g = 2, 4, 6, and 8 were detected. The method has also been used to study spin–lattice relaxation mechanisms within the $S = {}^5/_2$ ground state of Fe^{3+} in MgO.[9] Izen and Modine[10] described a combined MCD and EPR spectrometer which employed an EPR system operating in a standard reflection arrangement at 9, 24, and 35 GHz. The optical cavity was immersed in liquid helium within a split-coil superconducting magnet with optical access along the field direction. The CD equipment, similar to currently available commercial instruments, used photoelastic modulation to generate a circularly polarized light beam. It was shown that the MCD signal of the V^- center in MgO monitored at 625 nm could be quenched partially on application of a microwave field at magnetic fields corresponding to the $g_\parallel$ and $g_\perp$ values of the V^- center. There has been a recent revival of interest in the technique with its application to the study of defect sites in III–V semiconducting compounds, notably, the antisite defects in GaAs.[11] In spite of the great potential value of such an experiment, rather few results appear to have been reported using this technique, and no application to the study of metalloproteins has been reported.

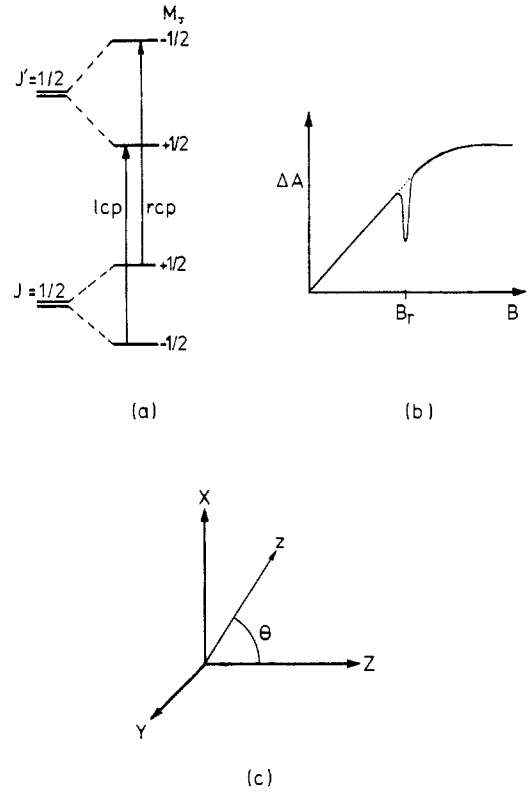

Figure 1. (a) Ground and excited electronic states of a paramagnetic system with $J = {}^1/_2$ in the absence and presence of a magnetic field. The allowed optical transitions when the light is propagated along the applied field are shown where LCP and RCP indicate left and right circularly polarized photons. (b) Plot of the intensity of the MCD signal, ΔA ($=A_{LCP} - A_{RCP}$), where A is absorbance, against applied magnetic field B at a temperature of, say, 1.5 K for the energy level scheme in (a). In the absence of microwave radiation, the curve is linear at low fields, becoming field independent at high fields. In the presence of a monochromatic microwave beam of energy $h\nu$, the MCD signal is partially quenched when the resonance condition $h\nu = g\beta B_r$ is fulfilled. (c) Axis system used for eq 1–7 in the text. Upper case letters refer to the laboratory frame, and lower case letters are the molecular frame.

The possibility of using a combined MCD microwave resonance experiment to study the paramagnetic centers in metalloproteins is an attractive one. It would enable each optical band in the electronic spectrum to be associated with a given g-value observed in the EPR spectrum. Furthermore, by measuring the MCD spectrum at a magnetic field at which microwave resonance occurs both in the presence of absence of an applied microwave field, the optical spectrum arising from a species with a given g value could be determined. Therefore we have designed and constructed an apparatus to investigate the optical detection of paramagnetic resonance by magnetic circular dichroism. We report the successful detection of such resonances from frozen aqueous solutions of Cu^{II}(EDTA) and from the blue copper protein azurin. Further we show how the analysis of the band shape of the ODMR spectrum of a paramagnetic species with an anisotropic ground-state g tensor can allow determination of the relative orientations of the principle axes of that tensor and those of the optical transition moment tensor. Thus, it becomes possible to measure the relative polarizations of the optical transitions of an isotropic solution of a metalloprotein. This appears to be the first report of the successful use of MCD spectroscopy for the optical detection of ground-state paramagnetic resonance of frozen aqueous solutions of proteins.

Principles of Measurement and Design of Apparatus

The principles involved in ODMR experiments are shown in Figure 1a, illustrated with a system with ground and excited states having effective spins of ${}^1/_2$ and placed in a static magnetic field B, parallel to the

(5) Greenwood, C.; Hill, B. C.; Barber, D.; Eglinton, D. G.; Thomson, A. J. *Biochem. J.* **1983**, *215*, 303.
(6) For reviews see: (a) *Triplet State ODMR Spectroscopy*; Clarke, R. H., *Ed.*; Wiley: New York, 1982. (b) Maki, A. H. In *Biological Magnetic Resonance*; Berliner, L. J., Reuben, J., *Eds.*; Plenum: New York, 1984; Vol. 6, Chapter 5. (c) Cavenett, B. C. *Adv. Phy.* **1981**, *30*, 475.
(7) Modine, F. A.; Izen, E. H.; Kemp, J. C. *Phys. Lett.* **1971**, *34A*, 413.
(8) Romestain, R. *C. R. Hebd. Seances Acad. Sci. Ser. B* **1969**, *269B*, 297.
(9) Cheng, J. C.; Kemp, J. C. *Phys. Rev. B.* **1971**, *4*, 2841.
(10) Izen, E. H.; Modine, F. A. *Rev. Sci. Instrum.* **1972**, *43*, 1563.
(11) Meyer, B. K.; Spaeth, J.-M.; Scheffler, M. *Phys. Rev. Lett.* **1984**, 52, 851.

laboratory z axis. Optical transitions between the ground and excited states are induced by right and left circularly polarized photons propagated along the magnetic field axis according to the selection rules $\Delta M_S = 0$ and $\Delta M_L = +1$ or -1, respectively. The intensity of the MCD signal is given by $\Delta A(=A_L - A_R)$ where A_L and A_R are the absorbances for left and right circularly polarized light. At a temperature of 1.5 K, the MCD intensity is almost wholly due to the Boltzmann population difference between the $M_J = \pm^1/_2$ Zeeman sublevels of the ground state. A plot of ΔA against the applied magnetic field B will vary as shown in Figure 1b. For a temperature of 1.5 K and a Zeeman splitting, $g\beta B$, of less than ~ 4 cm^{-1}, the variation of ΔA with B is linear, Curie law behavior. Magnetic saturation occurs at higher B values. Application of a microwave field of frequency $h\nu$ with its oscillatory magnetic field linearly polarized along x, B_1^x, will induce magnetic dipole transitions from $M_J = -^1/_2$ to $+^1/_2$ when the resonance condition $h\nu = g\beta B_r$ holds. The spin temperature of the system will be raised by an amount depending upon the microwave power level and the spin–lattice relaxation time. Thus, the MCD signal is quenched in part and the microwave-induced resonance will be observed on a plot of ΔA against B as indicated in Figure 1b.

In order to carry out such an experiment a frozen aqueous solution must be held at cryogenic temperature in a high Q microwave cavity which has optical access along the direction of the static field. A split-coil, reentrant top-loading superconducting magnets such as the SM-4 built by Oxford Instruments, PLC, is ideal for this type of experiment. A microwave guide terminating in a cavity, with optical access, can be lowered into the sample space. The cavity is immersed in liquid helium and can be pumped to ~ 1.5 K. The resonant frequency of the cavity is allowed to drift up as the temperature is lowered from room temperature to 1.5 K. The cavity is then matched to give maximum power input. Matching of the cavity to the waveguide is carried out from outside the cryostat.

MCD measurements are carried out in our laboratory, by using a JASCO J-500D spectropolarimeter fitted with the SM4 superconducting magnet. The magnet contains a Helmholtz pair of solenoids capable of generating a maximum field of 5 T along the axis midway between the coils. The field homogeneity is >1% over a sphere of 10-mm diameter at this point. This is not as high as would normally be used in a magnetic resonance experiment. However, since the line widths are much greater than the inhomogeneities this is not limiting. The sample space between the split pair is rectangular in cross section with strain-free optical windows normal to the field axis. This space can be filled with liquid helium from the main helium bath and pumped, independently of the bath, to a temperature of ~ 1.5 K. Access is from the top of the magnet cryostat via a long cylindrical tube of diameter 40 mm.

A rectangular cavity resonating in the Q-band frequency range has been designed. This frequency band was selected for a number of reasons. First, the restricted dimension of the sample chamber in the magnet dictated a high-frequency cavity if a conventional design was to be employed. Second, there is some advantage in using a resonant magnetic field as high as possible. This ensures that the MCD signal develops an intensity that can be detected with good signal-to-noise (S/N) at microwave resonance. Third, Q-band microwave circuit components are readily available. There is a potential disadvantage arising from the higher spin–lattice relaxation rate.

The cavity is a rectangular box formed from standard rectangular copper waveguide which resonates in the TE_{102} mode. The unloaded Q of the cavity is calculated to be 4000 and the loaded Q was measured to be 500 at 30 GHz.[12] Coupling is via a copper diaphragm with a hole diameter chosen to give critical coupling with the cavity at 4.2 K. The cavity can be matched to the external circuit by means of movable pins in the matching section that can be adjusted from the top of the cryostat. The rest of the microwave circuit is standard and simple; see Figure 2. The source is a Gunn oscillator capable of delivering 150 mW of peak CW power at 34 GHz. The insertion loss of the transmission line from the oscillator to the cavity is about 4 dB at 30 GHz. The power coupled into the cavity is given by $(1 - |\Gamma|^2)$ where $|\Gamma|^2$ is the power reflection coefficient[13] measured at approximately 0.1 in our experiments. The power into the cavity is then $\approx 0.9 \times 0.5W$ where W is the power at the top of the probe set by the variable attenuator. The oscillator can be run either continuously or amplitude modulated with a square wave, variable in frequency between 1 and 2 kHz.

The sample cell is a cylinder of internal diameter 2 mm and length 1 mm cut from Teflon. The ends of the cylinder are sealed with silica windows made from 0.25-mm quartz cover slips. Legs radiating from the long axis of the cylinder serve to position it within the cavity and to align it along the static magnetic field and optical axis of the superconducting magnet. The volume of the sample cell is 3 μL. The cell is filled via small holes in the barrel of the cylinder by using a fine syringe needle.

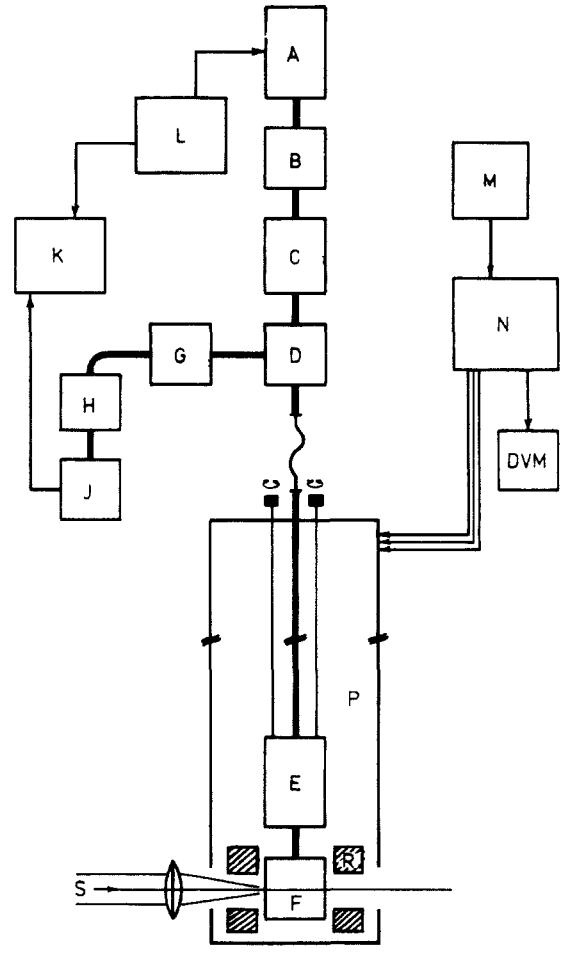

Figure 2. Schematic diagram of the microwave power circuit, the superconducting magnet system (SM4), and the magnet field scanning circuit for the MCD-ODMR experiment. The components are A, 29–36-GHz Gunn oscillator; B, isolator; C, 0–40-dB attenuator; D, 10-dB coupler; E, cavity matching section; F, cavity; G, 10-dB attenuator; H, wave meter; J, detector; K, oscilloscope; L, Gunn oscillator power supply; M, ramp generator; N, magnet power supply; DVM, digital volt meter; P, cryostat; R, superconducting magnet.

Optical access through the cavity is via two holes of diameter 2.0 mm drilled in opposite walls of the waveguide. Because the light beam from the monochromator of the JASCO-J500 spectropolarimeter has dimensions of 10 × 3 mm at the cavity, these holes constitute a serious stop in the optical system. In spite of this, remarkably good S/N ratios on the MCD signal were obtainable. Trials using an additional lens to focus the beam on the cavity optical port were attempted with some improvement in performance. The optical parameters in our apparatus are far from optimum and will be improved in future designs.

EPR spectra of all samples were measured both at X band, on a Bruker ER-200D spectrometer, and at Q band, with a Bruker ER051QR spectrometer, at 140 K. The Q-band spectra were integrated by computer to give the EPR absorption spectra. We thank Dr. J. F. Gibson (Imperial College of Science and Technology, University of London) for making the Q-band EPR measurements. Azurin (*Pseudomonas aeruginosa*) was purified by a standard method.[14]

Results and Interpretation

Cu^{2+}(EDTA). Cu^{2+}(EDTA) in aqueous solution and 50% (v/v) glycerol provided a convenient test of the equipment. The EPR spectrum measured at Q-band frequency in the absorption mode is given in Figure 5a. The g values estimated from the derivative mode spectra are $g_\parallel = 2.29$ and $g_\perp = 2.062$, in good agreement with the values of $g_\parallel = 2.337$ and $g_\perp = 2.090$ reported at X-band

(12) *Microwave Measurements*; Ginzton, E. L., Ed.; McGraw-Hill: New York, 1957; p 413.
(13) *Microwave Transmission Circuits*; Ragan, G. L., Ed.; McGraw-Hill: New York, 1948; MIT RLS-9, p 34.
(14) Ambler, R. P.; Brown, L. H. *Biochem. J.* **1967**, *104*, 784.

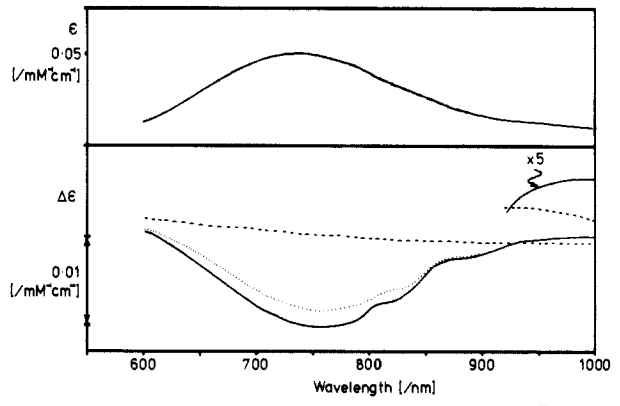

Figure 3. Absorption (upper) and MCD (lower) spectra of Cu^{II}(EDTA) in glycerol/water (50:50 v/v) at room temperature and 1.7 K, respectively: (---) zero magnetic field; (—) MCD at 1.16 T; (···) MCD at 1.16 T in the presence of 1.7 mW of microwave radiation at a frequency of 32.221 GHz. The frequency and field correspond to a g value of 2.062, the $g_\perp$ value for Cu^{II}(EDTA).

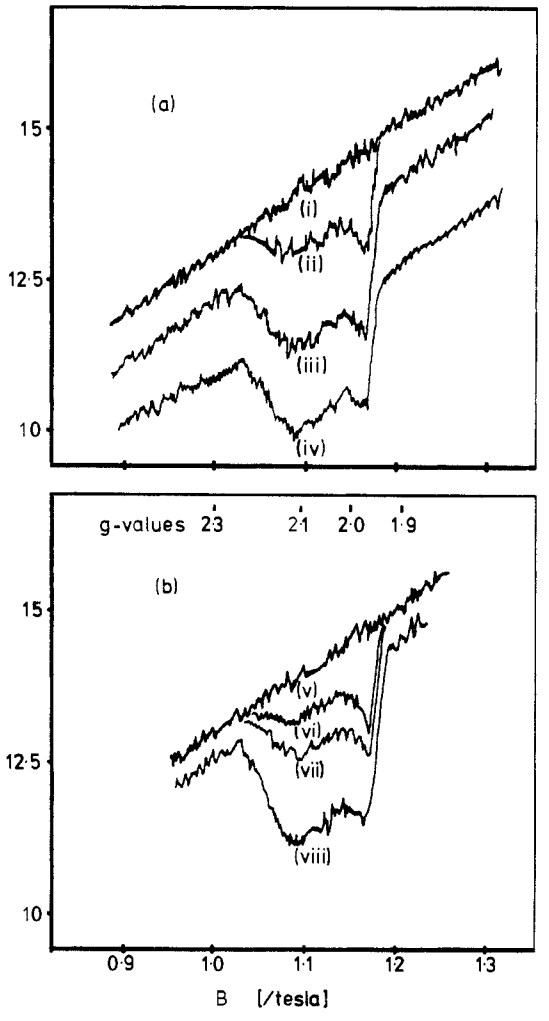

Figure 4. Magnetic field (B) dependence of the MCD intensity (ΔA) monitored at 740 nm of Cu^{II}(EDTA) in glycerol/water (50:50 v/v). Temperature = 1.7 K, microwave frequency = 32.221 GHz. (a) Continuous microwave power at (i) $<1 \times 10^{-4}$, (ii) 0.03, (iii) 1.88, and (iv) 7.5 mW. (b) Pulsed microwave power (duty cycle 4%) at (v) $<1 \times 10^{-4}$, (vi) 0.03, (vii) 0.12, and (viii) 7.5 mW.

frequency.[15] Copper nuclear hyperfine structure is not readily detected in the Q-band absorption mode EPR spectrum. The room-temperature absorption and low-temperature MCD spectra are given in Figure 3. The latter is, as expected, temperature

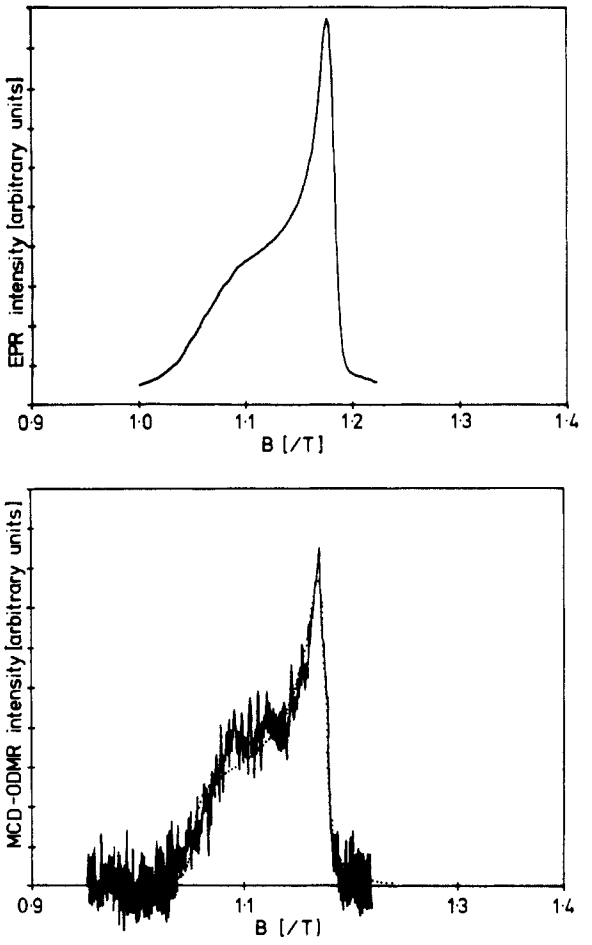

Figure 5. Comparison of the line shapes of the Q-band EPR and MCD-detected ODMR of Cu^{II}(EDTA). Sample conditions as in Figure 3. (a, top) Q-band EPR in the absorption mode. Temperature = 139 K, frequency = 34.02 GHz, power = 7 mW. (b, bottom) (—) MCD-ODMR derived from Figure 4b. Temperature = 1.7 K, frequency = 32.221 GHz, power = 0.1 mW pulsed, optical wavelength = 740 nm. (···) Computer-simulated MCD-ODMR line shape, using $B_\parallel = 1.075$ T, $B_\perp = 1.175$ T, Lorenzian line width = 3 mT, and $M_+ = 0.5$, $M_z = 0.5$.

dependent. The region of the spectrum shown, between 500 and 1000 nm, arises from d–d transitions of the Cu(II) ion. The intensity of the MCD spectrum at 740 nm without and with the application of a microwave field of frequency 32.221 GHz at 1.7 K is plotted in Figure 4. With no microwave field present, the MCD intensity ΔA is linearly dependent upon the magnetic field in the range 0.7–1.2 T as expected. In the presence of the microwave field, the MCD signal is partially quenched. The degree of quenching depends upon the microwave power applied, as shown in Figure 4. At the highest available powers, the band shape undergoes a change, suggesting that microwave saturation is being approached. It has been reported by others that ODMR signals are subject to line broadening at high applied microwave powers.[16] Experiments have been carried out with the microwave power applied continuously and in amplitude-modulated pulses. The application of continuous microwave power leads to a decrease in the MCD intensity even away from magnetic fields at which resonance occurs. It is likely that there is some heating of the frozen aqueous sample caused by dielectric interaction with the microwave electric field. Square-wave pulses of microwaves gave rise to this effect only at high microwave powers, lending support to this explanation.

The line shape of the ODMR spectrum was obtained with the data given in Figure 4 by differencing the intensity variation of the MCD signal with and without microwave power. The resulting difference spectrum is given in Figure 5a. There is good agreement

(15) Malstrom, B. G.; Vänngård, T. *J. Mol. Biol.* **1960**, *2*, 118.

(16) See ref 6a, Chapter 3, p 64.

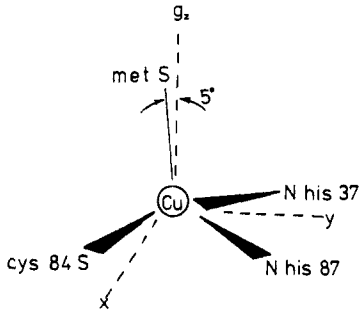

Figure 6. Coordination geometry of copper(II) in plastocyanin (*Populus nigra*) from ref 21. The geometry of azurin (*Pseudomonas aeruginosa*) is taken to be identical.

between the shapes of the EPR and ODMR spectra. As will be shown later, this suggests that the optical transition at 640 nm used to detect the ODMR spectrum has equal electric dipole intensity along all three g-tensor axes, x, y, and z. This is an unexpected finding since the EPR spectrum is anisotropic.

The MCD spectrum, Figure 3, has been recorded at a magnetic field of 1.16 T and at 1.7 K both in the presence and the absence of a microwave field of 32.221 GHz. The partial quenching of the MCD is clearly evident. It is uniform across the whole of the wavelength region 600–850 nm, showing that the optical transitions in this region are essentially isotropic. The degree of quenching of the MCD signal is only 10% even at maximum power when the magnetic field is set at the resonance field of the maximum intensity in the ODMR spectrum. The reason for this is that the bandwidth of the double-resonance cavity is narrow. With an effective figure of merit (Q) of 500, the bandwidth is 120 MHz at one-third the maximum height. Assuming a g value of 2, this is translated into a magnetic field width of ±2 mT. Since the ODMR spectrum is spread out over a total magnetic field width of 150 mT, only a small proportion of the total number of Cu^{2+}(EDTA) molecules is in magnetic resonance at any given magnetic field. However, the optical spectrum of a single Cu^{2+}(EDTA) molecule is very broad. All Cu^{2+}(EDTA) molecules contribute to the MCD spectrum at all wavelengths. Only a small proportion has their MCD spectrum quenched at any given resonant magnetic field. This factor may well be a fundamental limitation upon the sensitivity of the technique. Indeed it is rather surprising that ODMR spectroscopy is possible given that EPR line widths are narrower than optical line widths by factors of $\sim 10^6$, at least. It may be that more complete quenching of a MCD signal could be achieved by using a broader bandwidth of microwave irradiation. This would require a slow-wave helix or similar device. Thus, compared with conventional microwave spectrometers where narrow bandwidths are needed, the design requirements of the instrument appear to be rather different for ODMR spectroscopy.

Azurin (*Pseudomonas aeruginosa*). Azurin is a member of the so-called blue or Type 1 copper-containing class of proteins[17] with unique spectral features including an extremely intense absorption band ($\epsilon \sim 3$–5000 M^{-1} cm^{-1}) at ~600 nm with weaker bands at higher and lower energy and an axial EPR spectrum ($g_\parallel = 2.13$, $g_\perp \sim 2.05$) with small copper parallel hyperfine splitting ($A_\parallel < 63 \times 10^{-4}$ cm^{-1}).[18] Since the charge-transfer, ligand field spectra and EPR spectra of azurin are extremely similar to those of plastocyanin, a coordination site within the protein for the cupric ion of closely similar structure has been assumed. The X-ray crystallographic study of *Pseudomonas aeruginosa* azurin[19] assumes the same copper site coordination geometry as that determined by X-ray crystallography for the protein plastocyanin, from *Populus nigra*.[20] This structure has been refined to 1.6-Å resolution allowing determination of the copper atom coordination geometry to an estimated standard deviation of 0.02 Å. The copper atom is coordinated in a distorted tetrahedral geometry by the side chains of the cysteine and two histidines as well as methionine, Figure 6. Of importance for the work described here is the spectroscopic study of single crystals of *Populus nigra* plastocyanin in which polarized single-crystal optical and single-crystal EPR spectra are reported.[21] The approximate orientation of the ground-state g tensor with respect to the blue copper site has been determined. It has been shown that the unique axis of the g tensor, g_z, is oriented about 5° away from the copper methionine axis. The position of the $d_{x^2-y^2}$ orbital, which contains the unpaired electron, is estimated to be perpendicular to this axis. The polarized single-crystal electronic spectrum shows that most of the intensity of the spectrum between 500 and 800 nm is polarized approximately perpendicular to the copper methionine axis. Detailed assignments of the transitions within this wavelength range are made to change-transfer transitions from the cysteine sulfur thiol and the two histidine ligands. The polarization properties of the electronic spectrum bear out the evidence of the EPR g-tensor axial symmetry with the axis almost parallel to the copper methionine bond.

The MCD spectrum of azurin (*Ps. aeruginosa*) at 1.7 K and 1.06 T over the wavelength range 350–1000 nm is given in Figure 7 along with the room-temperature absorption spectrum. This sample contains a small amount of contamination from cytochrome c_{551} as evidenced by the peak at 410 nm in the absorption spectrum and the double-signed feature in the MCD at the same wavelength region. The shoulders at 550 nm in the MCD spectrum arise from the same chromophore. A sample of azurin freed from cytochrome contamination by fast protein liquid chromatography gives an absorption and MCD spectrum free from these features. We choose to show the experiments with the heme-contaminated sample in order to see whether optical features due to cytochrome and copper can be distinguished readily in the ODMR experiments. The level of cytochrome c_{551} impurity in the sample shown in Figure 7 is estimated to be ~5% from an inspection of the MCD signal intensities. This concentration of cytochrome could not be detected in the X-band EPR spectrum showing the superior sensitivity of low-temperature MCD spectroscopy for detecting low-spin ferric heme.

The ODMR spectra have been recorded at wavelengths of 640 and 1000 nm from the heme-contaminated sample of azurin. The results are shown in Figure 8b and 8c. The Q-band EPR spectrum of the same solution measured at 139 K is shown, in the absorption mode, in Figure 8a. A comparison of these three figures show that the ODMR spectra have shapes similar to one another but very different from that of the Q-band EPR spectrum. Qualitatively it can be stated that only the $g_\parallel$ component of the g tensor is being detected optically via the MCD transitions at 640 and 1000 nm. In an azurin sample free from cytochrome contamination similar results are obtained. In addition the ODMR spectra have been recorded at two additional wavelengths, 720 and 460 nm, and qualitatively similar line shapes to those of Figures 8b and 8c have been obtained. Detailed simulations of the shapes of the ODMR curves (see later) show that the transitions contributing to the MCD spectrum at these four wavelengths, namely, 460, 640, 720, and 1000 nm, are polarized perpendicular to the z axis of the g-tensor frame.

The MCD spectra recorded in the presence of microwave power at 1.06 T with the resonant magnetic field corresponding to the peak in the ODMR spectrum are shown in Figure 7. The MCD spectrum between 500 and 800 nm is partially quenched at a microwave frequency of 33.19 GHz and a magnetic field of 1.06 T. The microwave power delivered to the cavity is estimated to be 30 mW. This provides a quenching of 10% of the MCD signal at 1.7 K, corresponding to a rise in spin temperature of 1.9 K. A study of the power dependence of the signal quenching has not

(17) Malkin, R.; Malmstrom, B. G. *Adv. Enzymol.* **1970**, *33*, 177.
(18) For a review see: Gray, H. B.; Solomon, E. I. In *Copper Proteins*; Spiro, T. G., Ed.; Wiley: New York, 1981; Vol. 3, Chapter 1.
(19) Adman, E. T.; Jensen, L. H. *Isr. J. Chem.* **1981**, *21*, 8.
(20) Colman, P. J.; Freeman, H. C.; Guss, J. M.; Murata, M.; Norris, V. A.; Ramshaw, J. A. M.; Venkatappa, M. P. *Nature (London)* **1978**, *272*, 319.
(21) Penfield, K. W.; Gay, R. R.; Himmelwright, R. S.; Eickman, N. C.; Norris, V. A.; Freeman, H. C.; Solomon, E. I. *J. Am. Chem. Soc.* **1981**, *103*, 4382.

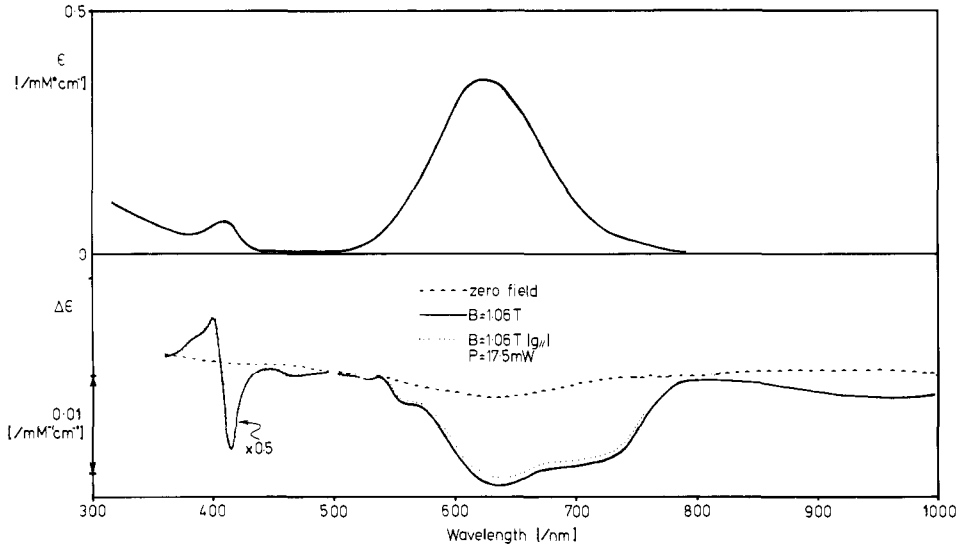

Figure 7. Absorption (upper) and MCD (lower) spectra of azurin (*Ps. aeruginosa*) in buffer/glycerol (50:50 v/v) at room temperature and 1.7 K, respectively. The buffer is 15 mM Hepes, pH 7.5 in D_2O. (---) Zero magnetic field, (—) MCD at 1.06 T, (···) MCD at 1.06 T in presence of 17.5 mW of microwave radiation at a frequency of 33.189 GHz, corresponding to a resonance at $g_\parallel = 2.29$.

been carried out. It is of interest that the MCD features due to cytochrome c_{551} between 350 and 500 nm are not affected by microwave irradiation at the same magnetic field that leads to partial quenching of the azurin peaks. The heme transitions throughout the visible and Soret bands are polarized in the x,y plane, the heme plane. Therefore these transitions should be detected in an ODMR experiment at magnetic fields in resonance with g_z of cytochrome c_{551}, that is ~3.0. We have been unable to detect either the ODMR spectrum of cytochrome c_{551} or any quenching of the MCD spectrum in the appropriate magnetic field range. The reasons for this are unclear but may be due to the much more rapid spin–lattice relaxation times of low-spin ferric heme compared with cupric ion. Therefore higher microwave source powers than are available either with a Gunn diode or a klystron at Q band may be required.

Simulation of the Line Shapes of ODMR Spectra. We consider the simulation of the MCD-detected ODMR spectrum of an axially symmetric paramagnet with a ground-state spin, $S = {}^1/_2$ having principle g values $g_\parallel$ and $g_\perp$. The ODMR spectrum is monitored by means of the MCD intensity at a fixed optical wavelength of an electronically allowed transition from the ground-state Kramers doublet $S = {}^1/_2$ to an excited state doublet $S' = {}^1/_2$. The optical transition can be x,y-polarized, z-polarized, or some combination of these two limiting polarizations. The principle axes of the optical transition moment tensor are taken to be the same as those of the g tensor. We are interested in simulating the spectrum of a frozen glass in which the molecules are assumed to be randomly oriented. Therefore we are deriving a "powder spectrum".

The calculation is carried out in the molecular frame x, y, and z which are also the ground-state g-tensor principle axes. The applied magnetic field, B, lies at an angle θ to z, Figure 1. The oscillating microwave magnetic field, B_1, is perpendicular to B. The circularly polarized light beam is propagated along B so that the electric vector of the light beam lies in the plane perpendicular to the field.

The ODMR spectrum is plotted as a function of applied magnetic field, B, between limits $B_\parallel$ and $B_\perp$ given by the resonance expression eq 1 where $h\nu$ is the energy (fixed) of the microwave source and β is the Bohr magneton, and $g(\theta)$ is given by the well-known expression eq 2. Hence, $B(\theta) = B_\parallel$ when $\theta = 0$ and $B(\theta) = B_\perp$ when $\theta = \pi/2$.

$$h\nu = g(\theta)\beta B(\theta) \tag{1}$$

$$g(\theta) = [g_\parallel{}^2 \cos^2\theta + g_\perp{}^2 \sin^2\theta]^{1/2} \tag{2}$$

Since the experiment is being performed at liquid helium temperature, the MCD intensity is dominated by the contribution of the C term.[4] At each value of the applied field, B, between $B_\parallel$ and $B_\perp$ and hence of θ, the intensity of the MCD C term is evaluated in the presence and absence of the microwave power by using the expression[22] eq 3. K is a proportionality constant

$$\Delta A(\theta) = KN(\theta)\Delta_{1/2}(\theta) \tanh\left[\frac{\Delta E(\theta)}{kT_i}\right] \tag{3}$$

$\Delta A = A_L - A_R$ where A_L and A_R are the absorption coefficients for left and right circularly polarized light, respectively. $N(\theta)$, the number of paramagnets or spins at an angle θ, is given by[23] eq 4. $\Delta_{1/2}(\theta)$ is the transition probability for the absorption of

$$N(\theta)\alpha[B(\theta)^3(1/B_\perp{}^2 - 1/B_\parallel{}^2)\cos\theta]^{-1} \tag{4}$$

differentially, circularly polarized light and can be expressed as eq 5 where $\bar{M}_+ = \langle {}^1/_2'|M_+|-{}^1/_2\rangle$, $\bar{M}_z = \langle {}^1/_2'|M_z|{}^1/_2\rangle$. (The primed M_S values refer to the excited electronic state.) $S = g_\parallel/g_\perp$ and $V = [\cos^2\theta(S^2 - 1) + 1]^{1/2}$. $\Delta E(\theta)$ is the Zeeman splitting given by (1).[22]

$$\Delta_{1/2}(\theta) = [\bar{M}_+{}^2(\cos^2\theta)S/V + 2^{1/2}\bar{M}_+\bar{M}_z(\cos^2\theta - 1)/V] \tag{5}$$

T_i is the temperature of the spin bath which in the absence of microwaves is the ambient temperature, T_0, of the liquid helium bath. In the presence of microwave power, the spin temperature is raised to T_S, as spins are pumped from $M_S = -{}^1/_2$ to $+{}^1/_2$ Zeeman sublevels. T_S therefore depends upon the microwave power absorbed and upon the spin–lattice relaxation time, τ_1. The probability, P, of absorption of microwave power by a paramagnet at an angle θ is given by[24] eq 6. $B_1{}^2$ is the microwave field intensity

$$P(\theta)\alpha q(\theta)B_1{}^2[(B - B(\theta))^2 + b^2]^{-1} \tag{6}$$

and depends upon $32QW(2f\upsilon)^{-1}$ where Q is the unloaded Q of the cavity, W is the transmitted microwave power, f is the microwave frequency, and υ is the cavity volume. $\{[B - B(\theta)]^2 + b^2\}$ is the Lorenzian line shape function where b is the line width at half height.

The EPR transition probability for a spin at θ is calculated from $q(\theta)$ which is a well-known expression[25] of the form of eq 7. Use

(22) Schatz, P. N.; Mowery, R. L.; Krausz, E. R. *Mol. Phys.* **1978**, *35*, 1537.
(23) *Electron Spin Resonance*; Wertz, J. E., Bolton, J. R., Eds.; McGraw-Hill: New York, 1972; p 156.
(24) Ibers, J. A.; Swalen, J. D. *Phys. Rev.* **1962**, *127*, 1914.

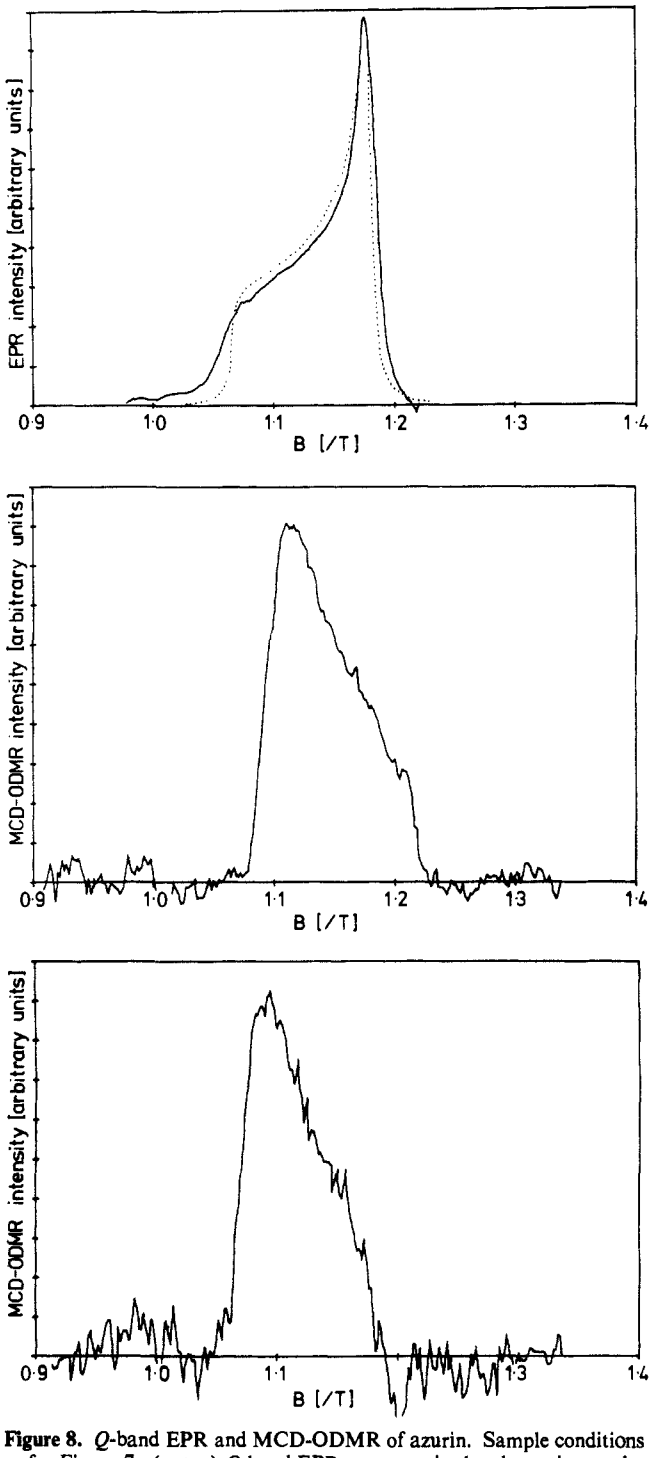

Figure 8. Q-band EPR and MCD-ODMR of azurin. Sample conditions as for Figure 7. (a, top) Q-band EPR spectrum in the absorption mode. Temperature = 139 K, frequency = 34.025 GHz, power = 7 mW: (—) experimental, (···) simulated curve (after Ibers and Swalen, ref 24) using $g_{\parallel} = 2.29$, $g_{\perp} = 2.06$, and Lorenzian width = 0.3 mT. (b, middle) MCD-ODMR monitored at an optical wavelength of 640 nm. Microwave frequency = 33.189 GHz, power = 17.5 mW, temperature = 1.7 K. (c, bottom) MCD-ODMR monitored at an optical wavelength of 1000 nm. Conditions as in (b).

of eq 6 and 7 enables the hyperbolic tangent in eq 3 to be calculated as in eq 8.

$$q(\theta) = \frac{1}{B_{\perp}^2}\left[\frac{B(\theta)^2}{B_{\parallel}} + 1\right] \tag{7}$$

$$\tanh\left(\frac{\Delta E(\theta)}{kT_S}\right) = \tanh\left(\frac{\Delta E(\theta)}{kT_0}\right)\{1 + 2P(\theta)\tau_1\}^{-1} \tag{8}$$

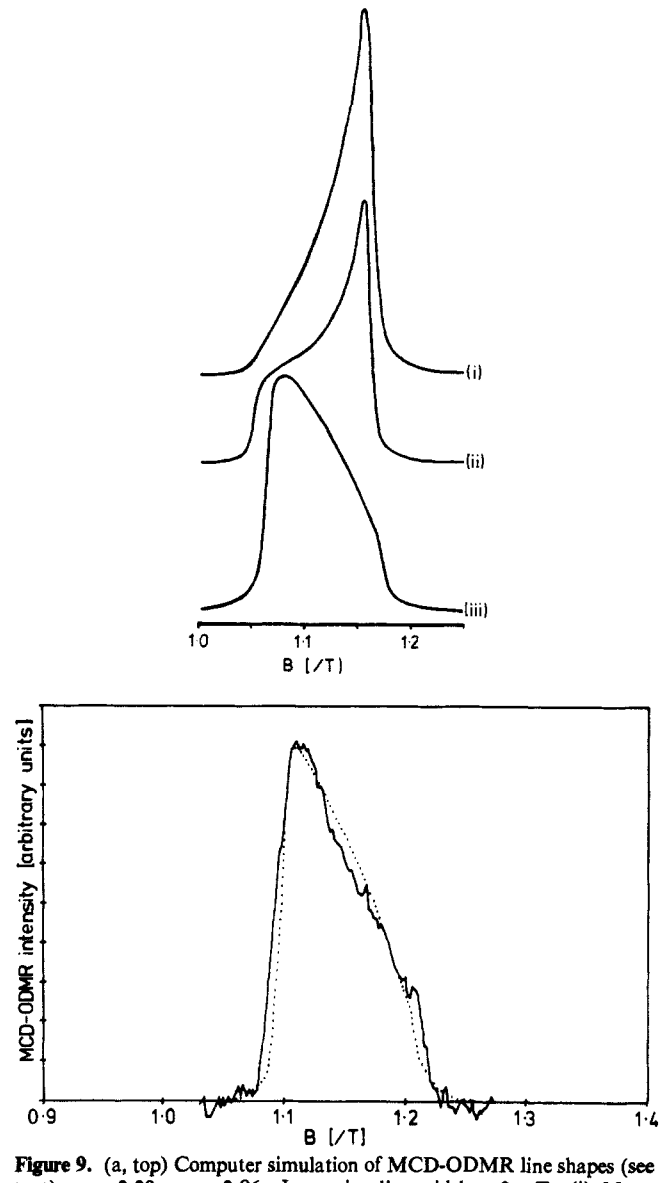

Figure 9. (a, top) Computer simulation of MCD-ODMR line shapes (see text), $g_{\parallel} = 2.29$, $g_{\perp} = 2.06$. Lorenzian line width = 3 mT. (i) $M_+ = 0.1$, $M_z = 0.9$. (ii) $M_+ = 0.5$, $M_z = 0.5$. (iii) $M_+ = 0.99$, $M_z = 0.01$. (b, bottom) Azurin MCD-ODMR data from Figure 8b and (···) simulation (see text) with parameters $g_{\parallel} = 2.29$, $g_{\perp} = 2.06$, Lorenzian line width = 3 mT, $M_+ = 0.995$, $M_z = 0.007$.

The assumption has been made that the spin–lattice relaxation time is field independent, which is reasonable for paramagnets with small g-value anisotropy.

A simple computer program has been written to generate ODMR spectra using the equations given above. Given values of $g_{\parallel}$ and $g_{\perp}$, the magnetic field limits, $B_{\parallel}$ and $B_{\perp}$, are evaluated. For a number of magnetic field points, usually 50, at equal field intervals between these two limits, θ is evaluated from eq 2. The parameters $P(\theta)$, $N(\theta)$, $\Delta_{-1/2}(\theta)$, and $\tanh(\Delta E(\theta)/kT_i)$ are easily evaluated via eq 6, 4, 5, and 8, respectively. The MCD intensity at each value of B, with and without microwave power, is then evaluated by using eq 3. Note that we do not calculate the absolute intensity of the MCD signal nor do we calculate the absolute magnitude of quenching of the MCD signal by the microwave power.

The transition probability for the absorption of circularly polarized light, eq 5, introduces into the ODMR lineshape a dependence upon the linear polarization of the optical transition being used to detect the paramagnetic resonance. For example, if M_z is zero, that is, the transition is purely x,y polarized, the second

(25) Bleaney, B. *Proc. Phys. Soc.* **1960**, *75*, 621.

term of eq 5 is zero. The ODMR lineshape obtained then is as shown in Figure 9a (iii). Only the $g_{\parallel}$ component of the g tensor is detected optically. This selectivity of the ODMR experiment when using MCD signals to detect the paramagnetic resonance arises because the circular polarized light is propagated along B, the applied magnetic field. A circular oscillator requires non-zero x and y components in the plane of the circle. If the optical transition is purely z polarized, then M_+ is zero, eq 5 is zero, and there is no ODMR signal. However, if the polarization ratio M_z/M_+ is large, say 10, so that the second term in eq 5 dominates, the ODMR line shape shown in Figure 9a (i) is observed and only the $g_{\perp}$ component of the g tensor is detected. For an isotropic transition, M_+^2 equals M_z^2 and the ODMR line shape, Figure 9a (ii), is equivalent to that of the absorption mode EPR spectrum. Hence for the simple case outlined here, namely, for an axially symmetric electronic system in which the principle axes of the ground-state g tensor and the optical transition moment tensor are parallel and the unique axes colinear, the ODMR line shape can be analyzed to determine the polarization of an optical transition relative to the g-tensor directions. It remains for future work to investigate line shapes which will arise for the case of rhombically distorted systems and for instances in which there is no symmetry determined relationship between the g-tensor and optical transition moment tensor axes.

Line Shapes of ODMR Spectra of Cu^{2+}(EDTA) and Azurin. Using the band-shape simulation procedure for isotropic and axial cases outlined in the preceding section, we have fitted the ODMR spectrum of Cu^{2+}(EDTA) monitored at 740 nm using a Lorenzian width of 3 mT, the width that adequately accounts for the absorption mode EPR spectrum, Figure 5a, g values of $g_{\parallel} = 2.2$ and $g_{\perp} = 2.0$, and an isotropic optical transition. The fit obtained shown in Figure 5b is good and points to the conclusion that the optical absorption band at 740 nm is isotropic. The signal-to-noise ratio is not adequate to determine whether copper nuclear hyperfine structure is present in the ODMR spectrum.

The first derivative mode Q-band EPR spectrum of azurin shows a small rhombic splitting in the $g_{\perp}$ region (data not shown) which is not apparent in the X-band spectrum. Recently Penfield et al.[26] have reported a small rhombic splitting, $g_x = 2.042$ and $g_y = 2.059$, in the Q-band EPR spectrum of spinach plastocyanin. However, the polarized crystal spectrum of plastocyanin[21] has been interpreted in terms of an axially symmetric site. We therefore make a preliminary interpretation of the azurin ODMR band shape based upon the assumption that the electronic structure of the cupric center approximates closely to one of axial symmetry. The ODMR line shapes of azurin at 640 and 1000 nm are, within experimental error, the same. They can be simulated, Figure 9b, with parameters of $g_{\parallel} = 2.29$ and $g_{\perp} = 2.06$, a Lorenzian line width of 3 mT, and optical polarizations of $xy = 0.99$ and $z = 0.01$. The width of 3 mT simulates well the absorption mode EPR spectrum of the protein determined at Q band, Figure 8a. Hence, we conclude that the optical transitions at 640 and 1000 nm are polarized perpendicular to the direction of $g_{\parallel}$. According to the single-crystal EPR results of Penfield et al.[21] on poplar plastocyanin, this corresponds to directions almost perpendicular to the copper methionine bond. The polarized optical spectra[21] show that the bands in the wavelength range 500–800 nm have polarization ratios similar to one another and with values consistent with transitions polarized perpendicular to the copper methionine direction. The polarized crystal spectrum of the band at 1000 nm was not reported in the study by Penfield et al.[21]. Hence, the ODMR results reported here and single-crystal study on plastocyanin[21] are in agreement as far as the polarization properties are concerned.

The band at 1000 nm can be assigned to a d–d transition. Taking over the model of Gray and Solomon[16] for plastocyanin in order to describe the ligand field transitions, the d–d transitions under the point group C_{3v} are $d_{xy} \rightarrow d_{x^2-y^2}$ (xy polarized), $d_{z^2} \rightarrow d_{x^2-y^2}$ (z polarized), and $d_{xz,yz} \rightarrow d_{z^2-y^2}$ (xy polarized). Gray and Solomon[18] suggest that the spectral region at ~1000 nm arises from a transition which is predominantly $d_{xz,yz} \rightarrow d_{z^2-y^2}$. The ODMR line shapes are consistent with this interpretation, showing that the optical transition is predominantly xy polarized.

The optical absorption bands of poplar plastocyanin between 450 and 800 nm have been resolved into four, numbered 2–5, with peaks at 468, 560, 606, and 749 nm, respectively.[21] The polarization ratios of these bands obtained from the single-crystal optical spectrum indicate that they are predominantly polarized xy, perpendicular to the g_z direction. Taking over this analysis for azurin, we see that the negative MCD features in the same wavelength regions as bands 2, 4, and 5 of plastocyanin, namely, 460, 640, and 720 nm, give ODMR spectra showing predominantly g_z and hence the optical components contributing to the MCD spectrum must be mainly x,y polarized. Again this is nicely consistent with the results of the polarized crystal spectrum of plastocyanin. The only band in the latter spectrum which is polarized along the direction of g_z is the band numbered 1, in the Penfield et al. notation,[21] at 428 nm. At this wavelength, the MCD spectrum of the cytochrome-free azurin sample shows no appreciable intensity. This suggests that the transition may be polarized purely along the copper methionine direction with no x or y components. A one-dimensional oscillator can have no C-term MCD intensity. For this reason, an optical transition polarized purely in one dimension cannot be detected with MCD-ODMR.

The optical absorption bands 2–5 have been assigned to charge-transfer transitions from the histidine and cysteine ligands to the cupric $d_{x^2-y^2}$ orbital. The MCD-ODMR results presented here show that virtually all the MCD intensity lies perpendicular to g_z. The model proposed by Solomon and Gray[18] for the cysteine-to-copper charge-transfer bands requires three transitions arising from the occupied sulfur p_x, p_y, p_z set transferring an electron into the copper $d_{x^2-y^2}$ orbital. From symmetry and overlap considerations, all three bands must be polarized along the sulfur–copper bond. However, in order to detect MCD-ODMR in the g_z region, the optical transitions must carry both x and y intensity. Therefore a unidirectional transition moment along the sulfur–copper bond appears to be insufficient. Charge transfer from other ligands, such as histidines 37 and 87, lying close to the x,y plane may be required. Thus, the MCD-ODMR results require some degree of mixing of the charge-transfer states arising from cysteine and histidines lying approximately in the basal plane. Our failure so far to detect any appreciable z-polarized transition intensity in the charge-transfer spectrum of azurin is of note in view of the rather long (2.9 Å) methionine–copper distance.[27]

We are in the process of exploring the application of the MCD-ODMR technique to a wider range of copper and other metalloproteins as well as to structurally well-defined inorganic models in order to establish the nature of the conclusions which can be drawn. There seems little doubt, however, that the techniques offer great promise for the study of the structures of metal centers in metalloproteins including the determination of the relative polarizations of the electronic transitions of randomly oriented samples.

Acknowledgment. A.J.T. and C. G. are grateful to the S.E.R.C. and the Royal Society for grants in support of this work. C. B. and J. P. are supported by the S.E.R.C. We thank Dr. B. Climber, Microwave Division, GEC-MEDL, Lincoln, U.K., and P. Wilson, British Telecom Laboratories, Martlesham Heath, U.K., for assistance with the development of the microwave cavity. Dr. J. F. Gibson, Imperial College of Science and Technology, University of London, London, generously measured Q-band EPR spectra. Thanks are due to Dr. R. Grinter and M. R. Cheesman for helpful discussions concerning the simulation of ODMR spectra.

Registry No. Azurin, 12284-43-4.

(26) Penfield, K. W.; Gewirth, A. A.; Solomon, E. I. *J. Am. Chem. Soc.* **1985**, *107*, 4519.

(27) Scott, R. A.; Hahn, J. E.; Doniach, S.; Freeman, H. C.; Hodgson, K. O. *J. Am. Chem. Soc.* **1982**, *104*, 5364.